

Document downloaded from:

<http://hdl.handle.net/10251/164159>

This paper must be cited as:

Gala, A.; Guerrero, M.; Serra Alfaro, JM. (2020). Characterization of post-consumer plastic film waste from mixed MSW in Spain: A key point for the successful implementation of sustainable plastic waste management strategies. *Waste Management*. 111:22-33.
<https://doi.org/10.1016/j.wasman.2020.05.019>



The final publication is available at

<https://doi.org/10.1016/j.wasman.2020.05.019>

Copyright Elsevier

Additional Information

1 **Characterization of post-consumer plastic film waste from**
2 **mixed MSW in Spain: A key point for the successful**
3 **implementation of sustainable plastic waste management**
4 **strategies**

5

6 Alberto Gala^{a,*}, Marta Guerrero^a, Jose Manuel Serra^b

7 *^aDepartment of Innovation, Technological Waste Innovation Centre (CIAM), URBASER*
8 *S.A., C/ Azufre 120, 50720 La Cartuja Baja (Zaragoza), Spain.*

9 *^bInstituto de Tecnología Química, Universitat Politècnica de València-Consejo*
10 *Superior de Investigaciones Científicas, Av. Los Naranjos s/n, 46022 Valencia, Spain.*

11

12 **Abstract**

13 The purpose of this paper is to provide a full characterization of post-consumer
14 plastic film recovered from mixed municipal solid waste (MSW) treatment plants in
15 Spain. Currently, this type of plastic waste is not recycled due to technical or
16 economic barriers and is still sent to landfill. Different types of municipal plastic
17 waste (MPW) from manual and automated sorting were studied: i) colour plastic film
18 recovered by ballistic separators and then manual sorting in different seasons; ii)
19 colour plastic film recovered by automated sorting (air suction); and iii) white plastic
20 film from primary manual sorting process. The samples were characterized by
21 different techniques, including the ultimate and proximate analysis, Higher Heating
22 Value (HHV) and Lower Heating Value (LHV), metal content, Thermogravimetric
23 Analysis (TGA) and Derivative Thermogravimetry (DTG), Fourier Transform
24 Infrared (FT-IR) analysis and Differential Scanning Calorimetry (DSC). The results

25 were compared to those obtained for pretreated colour and white plastic film waste
26 and contrasted with industrial recycled film granules of polyethylene (as a reference
27 material for packaging film). Additionally, pretreated plastic film samples were also
28 characterized by analysing viscosity, Pressure-Volume-Temperature (PVT) diagram,
29 specific heat capacity and halogen and sulphur contents. Characterization data from
30 this study will contribute to identify and develop potential recycling alternatives for a
31 more sustainable municipal plastic waste management, which is recognized as a
32 priority in the European Circular Economy Action Plan to use resources in a more
33 sustainable way.

34

35 *Keywords:* municipal plastic waste, sorting, plastic waste characterization, recycling,
36 circular economy.

37

38 *Nomenclature:*

39 Cp: Specific heat capacity [$\text{J}\cdot\text{g}^{-1}\cdot\text{°C}^{-1}$]

40 T5: Temperature at which 5 wt. % loss occurs in TGA/DTG analysis [°C]

41 T10: Temperature at which 10 wt. % loss occurs in TGA/DTG analysis [°C]

42 T50: Temperature at which 50 wt. % loss occurs in TGA/DTG analysis [°C]

43 T80: Temperature at which 80 wt. % loss occurs in TGA/DTG analysis [°C]

44 Tmax: Temperature at which maximum weight loss rate occurs in TGA/DTG analysis
45 [°C]

46 η : Dynamic viscosity of fluid [$\text{Pa}\cdot\text{s}$]

47 $\dot{\gamma}$: Shear rate [s^{-1}]

48 *Abbreviations:*

49 ACF: Colour plastic film recovered by automated sorting from MSW

- 50 ACF-W: Colour plastic film recovered by automated sorting from MSW - Season:
- 51 Winter.
- 52 CF: Colour plastic film recovered by manual sorting from MSW
- 53 CF-A: Colour plastic film recovered by manual sorting from MSW - Season: Autumn
- 54 CF-S: Colour plastic film recovered by manual sorting from MSW - Season: Summer
- 55 CF-SP: Colour plastic film recovered by manual sorting from MSW - Season: Spring
- 56 CF-W: Colour plastic film recovered by manual sorting from MSW - Season: Winter
- 57 CG: Granules obtained from colour plastic film recovered by manual sorting
- 58 DSC: Differential Scanning Calorimetry
- 59 DTG: Derivative Thermogravimetry
- 60 EU: European Union
- 61 FT-IR: Fourier Transform Infrared
- 62 HDPE: High Density Polyethylene
- 63 HHV: Higher Heating Value
- 64 ICP-OES: Inductively Coupled Plasma-Optical Emission Spectroscopy
- 65 IG: Industrial recycled film granules
- 66 LDPE: Low Density Polyethylene
- 67 LHV: Lower Heating Value
- 68 LLDPE: Linear Low Density Polyethylene
- 69 MDSC: Modulated Differential Scanning Calorimetry
- 70 MPW: Municipal Plastic Waste
- 71 MSW: Municipal Solid Waste
- 72 PE: Polyethylene
- 73 PP: Polypropylene
- 74 PVT: Pressure-Volume-Temperature

- 75 TGA: Thermogravimetric analysis
- 76 WF: White plastic film recovered by manual sorting from MSW
- 77 WF-S: White plastic film recovered by manual sorting from MSW - Season: Summer
- 78 WF-W: White plastic film recovered by manual sorting from MSW - Season: Winter
- 79 WG: Granules obtained from white plastic film recovered by manual sorting
- 80
- 81 *Corresponding author:
- 82 E-mail: ajgala@urbaser.com
- 83

84 **1. Introduction**

85 Nowadays, plastics are used for a large and growing variety of products, applications
86 and sectors, becoming an essential part of the daily life (Faraca and Astrup, 2019;
87 Hestin et al., 2015; Lopez, et al., 2017; Park et al., 2019; Wang et al., 2015). An
88 evidence of this is that the European plastic industry had a trade balance of more than
89 15 billion euros in 2018 (Plastics Europe, 2019a). At the same time, those
90 characteristics that make plastics so useful, such as durability, lightweight and other
91 intrinsic properties, also lead to challenging sustainable waste management (Wong et
92 al., 2017), and this is becoming more critical due to the continuous increase in the
93 amount of plastic waste. It has been estimated that about 10.6 wt. % of plastic waste
94 contributes towards the total municipal waste (Singh et al., 2019). The magnitude of
95 plastic waste problem can be surmised from plastic market data because many
96 applications are characterized by a short life (Lopez et al., 2017; Panda et al., 2010).
97 According to the latest data provided by Plastics Europe (2019a), total European
98 converter demand reached 51.2 Mt in 2018 and 3.9 Mt (7.6 %) corresponded to Spain.
99 Polypropylene (PP) and low-density polyethylene (LDPE) / linear low-density
100 polyethylene (LLDPE) were the most demanded polymer types in 2018. The major end-
101 user of this type of polymers is the packaging industry, which consumes the largest
102 share of plastics (39.9 % in 2018); and hence this industry is the most contributing to
103 the plastic waste stream, accounting for 61 % of the total post-consumer collected
104 plastic waste in Europe. This is partly because packaging plastics tend to have a shorter
105 lifetime than other plastic products (Achilias et al., 2007). In 2016, about 2.3 Mt of
106 post-consumer plastic waste was collected through official schemes in Spain (Plastics
107 Europe, 2018), of which 46.4 % was still sent to landfill. This value is above the
108 European average (24.9 %) (Plastics Europe, 2019a). Just as in Europe, the largest

109 volume of plastic waste collected through official schemes in Spain in 2016 was also
110 packaging waste (1.5 Mt) and landfill was the second treatment option for plastic
111 packaging waste in Spain, accounting for 38.2 % ([Plastics Europe, 2018](#)). According to
112 the waste hierarchy established by the Waste Framework Directive ([EU, 2008](#)), landfill
113 is the least preferred waste treatment option because of the serious environmental
114 impact and evident loss of resources. In this sense, EU policies are directed to transform
115 Europe into a more circular and resource efficient economy by adopting new directives,
116 aimed at achieving a maximum MSW landfilling of 10 % by 2035 (*i.e.* [EU, 2018](#)). To
117 accomplish this ambitious target, sustainable plastic waste management must play a key
118 role ([Circular economy strategy, 2019](#); [Yan et al., 2020](#)). Based on URBASER database
119 (multinational environmental service provider), the most common polymers in MPW in
120 Spain are polyolefin compounds: low-density polyethylene (LDPE), high-density
121 polyethylene (HDPE), polypropylene (PP) and linear low-density polyethylene
122 (LLDPE). Such polymers account for 67 % of the total post-consumer collected plastic
123 waste. Other polymers, accounting for 28.9 %, are mainly represented by polystyrene
124 (PS) (13.3 %), vinyl polychloride PVC (10.3 %) and polyethylene terephthalate PET
125 (5.3 %). At present, the main recycling route to recover the intrinsic value of plastics
126 relies on mechanical recycling ([Ellen MacArthur Foundation, 2016](#); [European
127 Parliamentary Research Service Blog, 2017](#); [Ragaert et al., 2017](#)). However, only two
128 types of plastic products recovered from mixed MSW are currently suitable for
129 mechanical recycling: HDPE and PET; any other type of municipal plastic waste is not
130 economically viable for mechanical recycling due to the lack of quantity (steady
131 production) and/or purity/quality due to the presence of particle and/or molecular
132 contamination (homogeneity) ([Dahlbo et al., 2018](#); [Faraca and Astrup, 2019](#)). It is thus
133 essential to consider new developments or innovations, e.g. chemical recycling, as

134 complementary recycling methods to mechanical recycling in alignment with the
135 European Commission's strategy ([Plastics Europe, 2019b](#)), especially for
136 LDPE/LLDPE (main components of packaging film) that makes up the greatest fraction
137 of municipal plastic waste and is still sent to landfill ([Dahlbo et al., 2018](#); [Diaz-
138 Silvarrey and Phan, 2016](#); [Horodytska et al., 2018](#); [Kunwar et al., 2016](#)). According to
139 several authors (e.g. [Bisinella et al., 2017](#); [Faraca and Astrup, 2019](#)), detailed
140 knowledge on the composition and impurities in plastic waste streams is a crucial point
141 to identify potential sustainable plastic waste management technologies to transform
142 plastic waste into a valuable new resource, for Life Cycle Assessment (LCA) of waste
143 management solutions and to support their successful commercial application (i.e.
144 pyrolysis), since there is a strong relationship between raw material composition and the
145 product quality/commercial value and yield ([Angyal et al., 2007](#); [Kunwar et al., 2016](#);
146 [Pinto et al., 1999](#)). Among these innovative recycling technologies, pyrolysis is
147 receiving renewed attention since it enables to directly transform plastics into very
148 valuable products with high potential to be used as fuel or petrochemical feedstock
149 ([Czajczyńska et al., 2017](#); [Khoo, 2019](#); [Sharuddin et al., 2016](#)). In this sense, leading
150 petrochemical sector companies are currently revealing an increasing interest in the use
151 of pyrolysis liquids from municipal plastic waste for the production of new plastics
152 (BASF, 2018; NESTE, 2018; REPSOL, 2020), which is a clear example of closed loop
153 in a circular economy practice.

154

155 Despite comprehensive knowledge on plastic waste characteristics can play a critical
156 role for further innovations and improvements in recycling technologies (including new
157 developments in chemical recycling), there is still very limited information about the
158 characteristics of plastic packaging waste and more studies should be performed on both

159 quantities and qualities of plastic waste streams (Dahlbo et al. 2018; Faraca and Astrup,
160 2019) in order to identify the major contaminants, which are significantly affected by
161 the type of sorting (Ruj et al., 2015).

162

163 In this context and considering that more than half of all post-consumer plastic waste is
164 collected via different mixed waste collection schemes (Plastics Europe, 2019b), the
165 overall aim of this paper is to provide a full characterization of real post-consumer
166 plastic film waste recovered by manual and automated sorting from mixed MSW in
167 Spain. This waste cannot be recycled due to technical or economic barriers and is still
168 sent to landfill. The influence of seasonality on plastic film waste quality is also
169 analysed. In addition, the results are compared to those obtained for pretreated plastic
170 film waste samples and contrasted with LDPE/LLDPE industrial recycled film granules
171 (as a reference material for packaging film). The comparative characterisation provides
172 a better way to give an overview of contamination and to identify major contaminants in
173 plastic film waste streams. This study will provide a valuable insight into plastic film
174 waste characteristics and thus will contribute to the commercial development of cost
175 and energy-efficient alternatives. Among them, pyrolysis seems to be one of the most
176 promising technologies. This novel use for post-consumer plastics pave the way
177 towards a circular economy in the plastic sector.

178

179 **2. Materials and methods**

180 *2.1. Selection of materials*

181 The focus of this work is on post-consumer plastic film originating from household
182 waste in Spain and collected as part of mixed MSW. According to the guide published
183 by the Waste and Resources Action Programme (2016), packaging film waste produced

184 by households comprise carrier bags and packaging of a large range of domestic
185 products. Although there are different types of polymers used to produce film packaging
186 due to the variability in packaging film characteristics ([Balakrishnan et al., 2014](#); [Waste
187 and Resources Action Programme, 2016](#)), polyethylene (PE) is the most common one
188 (derived from [British Plastics Federation](#) website). LDPE is widely used for utility bags
189 with moderate strength and stretch properties. LLDPE is employed for food bags,
190 newspapers bags, shopping bags and garbage bags. HDPE is also an excellent material
191 for manufacturing carrier bags and food wrapping material. Plastic film waste from co-
192 mingled streams is generally recovered by ballistic separation or air separation at MSW
193 treatment plants in Spain. The use of suction systems to extract these lighter materials
194 from a co-mingled stream does not separate the individual 2D material types, meaning
195 plastic film may be contaminated by paper and cardboard materials, as well as other
196 light materials such as PET bottles. In this study, two types of municipal plastic waste
197 from manual sorting were studied: 1) colour plastic film obtained from 2D flat and light
198 materials which are conveyed to the upper part of ballistic separators and then recovered
199 through manual sorting (CF); 2) white plastic film recovered from primary sorting
200 process in which bulky materials are manually separated in a closed booth (WF). The
201 waste sampling activities were carried out at the Zaragoza MSW treatment plant
202 according to CEN/TR 15310-3:2006 ([CEN, 2006](#)). Regarding colour plastic film, the
203 sampling activities were carried out during week days in the four seasons of a year.
204 White film sampling was conducted during the winter and summer seasons. In order to
205 assess the influence of manual/automated sorting systems on the quality of plastic film
206 recovered from mixed MSW, post-consumer plastic film waste recovered by suction
207 system (ACF) was also studied. These samples were taken in winter season from one of
208 the mechanical-biological sorting plants of Madrid. Despite plastic film is separated as a

209 positive flow, mixtures of polyolefins are too difficult to separate into mono-materials
210 streams (Mastellone, 2019) and a pretreatment step is necessary for chemical recycling
211 technologies like pyrolysis (Oasmaa et al., 2020). Taking this into account, colour and
212 white film waste samples from manual sorting were pretreated using conventional
213 methods (optical sorting, shredding in flakes having a size of 40 mm, wet cleaning and
214 drying) and then clean flakes were feeding into an extruder to produce a granulated
215 material. Colour and white film waste granules (CG and WG, respectively) were also
216 fully characterized and their properties were compared to those of colour and white film
217 waste samples. LDPE/LLDPE industrial recycled film granules (IG), used as a reference
218 material for packaging film (Abraham et al., 1992), were also characterized and their
219 properties were further contrasted.

220

221 2.2. *Characterization of plastic film waste samples*

222 The characterization of the different plastic film waste samples was performed by the
223 “Alfonso Maíllo” Technological Waste Innovation Centre (CiAM) at Urbaser
224 (Zaragoza), in collaboration with AIMPLAS (Plastics Technology Centre from
225 Valencia) and ITENE (Technological Centre in packaging, logistics, transport and
226 mobility from Valencia). Samples studied and characterization techniques used are
227 summarised in [supporting information](#). Table 1 shows the standards and commercial
228 equipment used for analysing chemical composition, heating values (Higher Heating
229 Value -HHV, and Lower Heating Value -LHV), metal content, Differential Scanning
230 Calorimetry (DSC) analysis and halogen content. Detailed description of each technique
231 is shown in [supporting information](#). The methodology followed for the rest of
232 characterization parameters is described below.

233

234 Thermogravimetric analysis (TGA) and Derivative Thermogravimetry (DTG) analysis
235 were used to study thermal stability. A *TA Instruments Q5000 IR* was used for the
236 measurement of weight change as a function of temperature. Samples were heated under
237 nitrogen flow ($100 \text{ mL} \cdot \text{min}^{-1}$) from 25 to $800 \text{ }^\circ\text{C}$ at a heating rate of $10 \text{ }^\circ\text{C} \cdot \text{min}^{-1}$.
238 Additionally, DTG curve (rate of change of weight) was used to aid interpretation. In
239 this regard, temperatures corresponding to maximum degradation rates (T_{max}) were
240 determined from the DTG plots. Fourier Transform Infrared (FT-IR) spectroscopy
241 analysis was carried out in a *TENSOR-27 FT-IR Spectrometer* with ATR crystal from
242 *BRUKER* in order to analyse the compositional functional groups and to identify
243 organic, polymeric and inorganic materials. Characteristic absorption bands were
244 obtained from 64 scans at a resolution of 4 cm^{-1} , in the mid-infrared wavenumber range
245 of 4000 to 600 cm^{-1} . The determination of viscosity was performed using an *AR-G2*
246 magnetic bearing, rotational rheometer (*TA Instruments*) with a 25 mm parallel plate
247 measuring system. Continuous flow tests were performed at 260, 270, 280 and $300 \text{ }^\circ\text{C}$
248 over the shear rate range of 0.001 - 1000 s^{-1} under nitrogen atmosphere. The rheological
249 model based on the Cross Equation ([Cross, 1965](#)) was used for extrapolating viscosity
250 data (η) as a function of shear rate ($\dot{\gamma}$). The effects of pressure and temperature on the
251 specific volume (PVT diagram) were studied using a *HAAKE PVT-100* apparatus,
252 which is based on the piston-die technique. The isobaric cooling mode was used by the
253 piston-die dilatometer in the temperature range from 50 to $200 \text{ }^\circ\text{C}$. The specific volume
254 was recorded along isobars from 200-1000 bar, with a fixed cooling rate of $5 \text{ }^\circ\text{C} \cdot \text{min}^{-1}$.
255 The specific volume at atmospheric pressure was obtained by Tait correlation ([Dymond
256 and Malhotra, 1988](#)). IKV model ([Boyard and Delaunay, 2016](#)) was used to describe the
257 dependence of specific volume on temperature and pressure. A *TA Instruments Q2000*
258 DSC was used to measure specific heat capacity using Modulated Differential Scanning

259 Calorimetry (MDSC). The conditions used were: i) modulation period of 80 s; ii) heating
260 rate of 1 °C·min⁻¹; and iii) temperatures from 50 to 320 °C. Sulphur content at trace
261 level was determined by oxidative pyrolysis and UV fluorescence detection, using a
262 *Mitsubishi TS-100/SD-100*.

263

264 **3. Results and discussion**

265 *3.1. Ultimate and proximate analysis and heating values*

266 Table 2 reports the results of the ultimate and proximate analysis along with the heating
267 values of the different types of post-consumer plastic film waste studied. Results for
268 industrial recycled granules (IG) are also included as a reference for polyethylene.
269 Oxygen content was determined by the difference between the sum of the weight
270 percentages of C, H, N, S and ash (on a dry basis) subtracted from 100. The results of
271 ash content on a dry basis are also included in Table 2. Likewise, the values of H/C ratio
272 on a molar basis were also calculated and shown. For colour film waste samples from
273 manual sorting (CF) samples, carbon was found to be in the range of 69-77 %, hydrogen
274 was about 11-12 %, nitrogen was less than 2 %, oxygen reached values up to 6 % and
275 sulphur content was negligible. According to carbon and hydrogen values, the energy
276 contents were remarkably high (HHV: 36366-42394 kJ/kg; dry basis), as expected since
277 PE is the major component. The ash content varied from 8.7 to 13.1 % (dry basis). This
278 fact is indicative of the presence of 2D materials different from PE (e.g.
279 paper/cardboard). Proximate analysis reported values of moisture content in the range of
280 11-15 %. The volatile matter was about 73.4-81.2 % and fixed carbon varied from 0.1 to
281 0.9 %. No clear influence of seasonality on plastic waste quality has been observed, as
282 sorting was carried out by hand-picked after the ballistic separator. Colour film waste
283 recovered by automated sorting (ACF-W) (automated sorting) exhibited higher oxygen

284 (11.8 %) and fixed carbon (3.3 %) values compared to those obtained from manual
285 sorting (CF), as well as lower H/C ratio. These observations may be attributed to the
286 presence of PET in waste coming from automated sorting, which is consistent with the
287 use of air separation system for film fraction recovery. Note that PET as an individual
288 component consists of around 30 % oxygen content and 6 % fixed carbon (Diaz-
289 Silvarrey and Phan, 2016). The presence of PET is also corroborated by DSC results
290 (see section 3.4). White film (WF) presents higher carbon and hydrogen contents (80-81
291 % and 13-14 %, respectively) in comparison with colour film waste samples (CF).
292 Therefore, their heating values (HHV > 43500 kJ/kg; dry basis) and volatile matter (>
293 92 %) are also higher. It is also remarkable that oxygen (< 3 %), ash (< 5 %) and
294 moisture contents (3 %) are much lower in WF. These observations reveal that WF
295 contains less undesired materials than CF and has a higher quality and potential to be
296 used directly as a source of fuels and chemicals. Note that the chemical composition of
297 WF is very close to that found in industrial recycled film granules (IG). For colour and
298 white film waste granules (CG and WG, respectively), the contents in carbon and
299 hydrogen are larger compared to CF and WF. This fact is due to the removal of
300 undesired materials (e.g. paper/cardboard, organic fraction, PET, etc.) attained through
301 the pretreatment process. The increase in carbon and hydrogen percentages is
302 accompanied with an increase in the heating values. Although there are no significant
303 differences between CG, WG and IG, it is interesting to note that the percentages of
304 carbon, hydrogen and volatile matter are slightly lower in CG. The ash content is higher
305 in CG in contrast with WG and IG (5.4, 1.0, and 1.0 %, respectively). Considering that
306 undesired materials (e.g. paper/cardboard, abrasive materials, PET, etc.) were
307 practically removed during the waste pretreatment, the higher ash content observed in
308 CG may be indicative of a higher presence of PP in colour film waste granules. This is

309 in agreement with [Dwivedi et al. \(2019\)](#) that reported that the ash content in PP is much
310 higher than that found in other municipal plastic waste, including PE, PET or PS. As
311 expected, the ash content in CG and WG was lower than that found in untreated
312 samples (CF and WF, respectively).

313 It is important to notice that ultimate analysis and heating values are key data in order to
314 set out mass and energy balances and subsequently to design new recycling processes.

315 In addition, the absence of oxygen and the relatively low values of fixed carbon make
316 post-consumer film especially suitable for pyrolysis technologies. In addition, volatile
317 matter confirms this hypothesis, i.e. the higher volatile matter in plastics being
318 pyrolyzed, the higher the yield of liquid products (Al-Salem, 2019).

319

320 *3.2. Metal content*

321 Table 3 reports the results of the metal content in all post-consumer plastic film waste
322 samples, including metals in industrial recycled film granules (IG) as a point of
323 reference. The typical elements found in a variety of plastic materials are listed in
324 [supporting information](#). Metal-containing compounds are present in additives that are
325 used for improving processability, stability or mechanical properties of polymers. As
326 has been reported elsewhere ([Ambrogi et al., 2017](#)), there are different types of
327 additives, including protective additives (antioxidants, photo-stabilizers, heat stabilizers
328 and flame retardants), mechanical properties modifiers (plasticizers and impact
329 modifiers), dyes and pigments, compatibilizers and fillers (the most used additives). In
330 addition, the presence of undesired materials in post-consumer plastic film waste may
331 also contribute to increase the content in metals. As can be seen in Table 3, calcium is
332 the most abundant element detected in all of the samples under study. Calcium is widely
333 employed in a variety of plastics as a filler (mainly as calcium carbonate; calcium

334 silicate) and photo-stabilizer (e.g. calcium-zinc and organo-calcium compounds), and,
335 to a lesser extent, as an antacid, lubricant (e.g. calcium stearate) or to increase resistance
336 to impact, stress and compression (e.g. calcium sulphate). The concentration of this
337 element is much higher in colour film samples from manual sorting (CF), exceeding the
338 value of 30000 mg·kg⁻¹. This finding could be due to the presence of HDPE in a higher
339 proportion, based on results reported in the literature. [Scott and Granchell \(2013\)](#)
340 reported that the calcium content in HDPE bottles is 93903 mg·kg⁻¹, which is higher
341 than that observed by [Sarker and Rashid \(2013\)](#) for LDPE (963 mg·kg⁻¹). The high
342 concentration of calcium may also be attributed to the presence of paper, since calcium
343 carbonate is used in paper mills as a filler material in the alkaline papermaking process
344 ([Hubbe and Gill, 2016](#)). It is important to note that relatively high concentrations of Al,
345 Fe, K, Na, Mg, Ti, Si, P and Zn were also detected in all the materials. High
346 concentration of Al may be attributed to the presence of aluminium trihydroxide
347 commonly used as a flame retardant. Aluminium silicate is also used as an additive in
348 polymers for increasing chemical resistance. High levels of Fe come from inorganic
349 pigments in the form of iron oxide or sulphide. K and Na may originate from additives
350 used mainly as thermal stabilizers (e.g. mica). Some K-compounds such as orthoclase
351 are also used for enhancing chemical resistance. Sodium benzoate is employed as a
352 nucleating agent in PP production. The high level of Na may suggest the presence of
353 this type of polymer in colour plastic waste samples from manual (CF) and automated
354 sorting (ACF). This is in agreement with the high sodium content found for PP by
355 [Sarker and Rashid \(2013\)](#) (5966 mg·kg⁻¹). The presence of PP in CF and ACF samples
356 is also supported by DSC results (see section 3.4). The common use of hydrated
357 magnesium silicate as a filler is the probable cause for the high concentrations of Mg
358 and Si detected, particularly in colour film plastic waste from manual sorting (CF). High

359 concentrations of Ti were also found due to its use as an inorganic pigment in the form
360 of titanium dioxide (white colour). Likewise, rutile titanium oxide is one of the most
361 effective and commonly used light absorbers. The presence of Ti may also be attributed
362 to catalyst residues from polymerization process. Organophosphorus antioxidants and
363 phosphorus-based flame retardants may be responsible for the high concentration of P
364 detected in plastic waste. Zn detected at concentrations up to about 400 mg·kg⁻¹ in
365 colour film obtained from manual sorting (CF) is mainly attributed to the use of both
366 Zn-based pigments (e.g. zinc oxide, zinc chromate) and heat stabilizers (e.g. zinc-based
367 salts, zinc carboxylate). Pb, Sn, Cr, Cu, Ba have also been detected, particularly in CF.
368 These elements are used in a number of pigments (in the form of oxides and sulphides)
369 and heat stabilizers (in the form of metallic salts, carboxylates, mercaptans and
370 sulphides). The data obtained from both colour and white film samples (CF and WF,
371 respectively) recovered by manual sorting (Table 3) reveal that there is no a significant
372 influence due to seasonal variations. However, the type of sorting (manual or
373 automated) plays an important role. As can be observed, higher concentrations of Ca, K,
374 Mg, P and Ti are found in CF (manual sorting) compared with ACF-W (automated
375 sorting). This fact may suggest the presence of a greater fraction of paper/cardboard in
376 samples obtained from manual sorting, since those elements are widely used as
377 additives in alkaline papers (e.g. calcium carbonate, mica, talc, titanium oxide,
378 phosphates esters etc.). This observation is in agreement with ash content results (see
379 [Table 2](#)). During the conditioning process, undesired components (e.g. paper/cardboard,
380 metal, glass, etc.) were removed from waste, decreasing the content of some elements.
381 Table 3 reveals that the concentration of some metals such as Al, Ca, Fe, K, Mg, Na and
382 P -present in paper/cardboard additives ([Hubbe and Gill, 2016](#))- is minor in CG
383 compared with CF. It is interesting to note that metals in colour film waste granules

384 (CG) are similar to those found in industrial recycled film granules (IG). Regarding the
385 metal content, the main differences between colour and white film waste granules (CG
386 and WG, respectively) are found in the contents of Ca and Fe. The concentration of
387 these elements is higher in the case of CG. It is also interesting to point out that the total
388 content of metal in colour film (CF) reaches values ranging from 2.9 to 5.2 %, whereas
389 the metal content in white film samples (WF) is significantly lower, around 1-2 %. This
390 is in agreement with the results of ash content reported in [Table 2](#). Also it is noteworthy
391 to indicate that some metals promote the thermo-oxidative degradation of plastic
392 materials (e.g. Fe, Co, Ni, Mn, Ti, V and Cu) ([Gorghiu et al., 2004](#); [Ojeda, 2013](#)).
393 Special attention should also be paid to the concentration of some elements (e.g. Si, Ca,
394 K, Na, Fe, P, V, Ni and As), especially when plastic waste is going to be used as a raw
395 material in catalytic processes, since they act as poisons for catalysts, decreasing their
396 activity and lifetime ([Argyle and Bartholomew, 2015](#)). Consequently, if the materials
397 are going to be used in catalytic pyrolysis, a pretreatment step may be essential.

398

399 *3.3. Thermogravimetric Analysis (TGA) and Derivative Thermogravimetry (DTG)*

400 *results*

401 TGA/DTG curves of CF-W, ACF-W, CG, WG and IG materials are displayed in Fig 1.
402 Detailed data are listed in Table 4. T5, T10, T50, T80 and Tmax represent the
403 temperatures at which 5 wt. %, 10 wt. %, 50 wt. %, 80 wt. % and the maximum weight
404 loss rate occurred, respectively. According to E2550-17 ([ASTM International, 2017](#)),
405 the onset temperature was determined by selecting the point on the TGA curve where
406 deflection is first observed from the established baseline prior to the thermal event. It
407 can be observed that the thermal decomposition of the industrial recycled film granules
408 (IG), used as a reference material for packaging film, starts at approximately 350 °C and

409 the main devolatilization takes place in the range of 450 and 500 °C. This fact is in
410 agreement with results reported in the literature related to polyethylene devolatilization
411 under nitrogen atmosphere, occurring in a single step (Diaz-Silvarrey and Phan, 2016;
412 Heikkinen et al., 2004; Kumar and Singh, 2011). In addition, it can be noted that the
413 char content is about 3.5 % (remaining solid at 800 °C). DTG data show that the
414 temperature corresponding to maximum degradation rate (T_{max}) of IG is 485 °C. The
415 degradation onset temperatures of colour film waste from manual and automated sorting
416 (CF-W and ACF-W, respectively) were displaced to the range of 185 °C. The DTG
417 curve of CF-W shows that there are three separate steps of devolatilization (Fig. 1b). It
418 can be stated that the first step, occurring at temperatures ranging from 250 to 380 °C
419 with a T_{max} of 336 °C, may be correlated with paper/cardboard devolatilization
420 (Alvarenga et al., 2016). The second step was observed in the range of 395-505 °C,
421 presenting the maximum rate of weight loss at 476 °C. Comparing TGA/DTG curves of
422 CF-W with IG, it can be concluded that this step is mainly associated with polyethylene
423 devolatilization, but minor presence of other types of polymers (e.g. PP, PS, PET) or
424 lignocellulosic materials may be probably present due to the broad band observed
425 (Heikkinen et al., 2004). It should be noted that PP has been detected in DSC results
426 (see section 3.4). The third devolatilization step is detected at temperatures of 625-650
427 °C, which may be attributed to silica dehydroxylation or thermal decomposition of
428 carbonates or aluminates (Pereira et al., 2017). It may also be due to the presence of
429 pigments/dyes or other types of additives (Alvarenga et al., 2016). The char content in
430 CF-W is much higher than IG (13.5 % vs. 3.5 %), confirming the presence of undesired
431 materials (mainly paper/cardboard) in plastic waste recovered by manual sorting. ACF-
432 W (automated sorting) presents a devolatilization step at a T_{max} of 345 °C, which may
433 be attributed to the presence of organic or lignocellulosic fractions. It can also be

434 observed two decomposition stages, partially overlapped in the range of 395-505 °C.
435 The DTG peak at 480 °C is due to polyethylene degradation, whereas the lower DTG
436 band may be probably accounted for the presence of PET in accordance with DSC
437 analysis. Results in literature show that T_{max} of PET occurs at about 434-441 °C
438 (Hujuri et al., 2008; Pereira et al., 2017). Hujuri et al. (2008) already suggested that
439 substituted/branched polymers like PET or PP degrade at lower temperatures than linear
440 polymers (LLDPE/LDPE/HDPE). However, it is important to point out that the weight
441 loss may also be due to lignocellulosic materials since lignin degradation occurs in the
442 temperature range of 250-500 °C (Lafia-Araga et al., 2012). The char content in ACF-W
443 is lower than that detected in CF-W (8 % vs. 13.5 %, respectively). This observation is
444 consistent with the values of ash content reported in Table 2, revealing that samples
445 from automated sorting contain less paper/cardboard than those recovered by manual
446 sorting. TGA-DTG curves for granules obtained from colour and white film waste (CG
447 and WG, respectively) are similar to those obtained for IG, suggesting that the major
448 component of both materials is polyethylene. The char content in CG is equal to that
449 detected in IG (3.5 %). For WG, no appreciable char content was observed at 800 °C.
450 Note that the DTG peak height at any temperature gives the rate of weight loss. In this
451 sense, it can be observed in Fig. 1b that CF-W (manual sorting) presents the lowest rate
452 of degradation, followed by the ACF-W (automated sorting). CG, WG and IG materials
453 have high rates of degradation, especially at temperatures above 450 °C. Thermal
454 stability increases after the pretreatment of plastic waste due to the removal of undesired
455 materials, mainly organic and lignocellulosic fractions. As can be seen in Table 4,
456 thermal stability increases after the pretreatment of plastic waste due to the removal of
457 undesired materials, mainly organic and lignocellulosic fractions. For example, it is
458 worth to note that T₅ increases from 226-289 °C for untreated plastic wastes (CF-W and

459 ACF-W, respectively) to temperatures above 400 °C for CG (404 °C) and WG (424 °C).
460 The fact that CG shows a lower thermal stability than WG reveals that PP content is
461 higher in CG, since PET and undesired materials were largely removed during the
462 pretreatment. All this information related to thermal stability and degradation rates is
463 essential to design thermochemical technologies because it is directly related to the
464 operational temperatures or reactors, especially in energy optimized processes in which
465 energy efficiency is a key point to maximise the process sustainability.

466

467 3.4. *Fourier Transform Infrared (FT-IR) spectroscopy and Differential Scanning* 468 *Calorimetry (DSC) analysis*

469 In order to obtain detailed information about compositional functional groups, post-
470 consumer plastic waste from manual and automated sorting (CF-W and ACF-W,
471 respectively) and pretreated samples (CG and WG) were examined using FT-IR
472 spectroscopy in the mid-infrared range (4000-600 cm^{-1}). Industrial recycled film
473 granules (IG) were also analysed by FT-IR as a reference for polyethylene. Results from
474 FT-IR also allow identifying the presence of organic, polymeric and inorganic
475 materials. As has been previously indicated (see section 2.1), plastic film waste mainly
476 consists of polyethylene because is the main polymer used to produce packaging film.
477 Therefore, characteristic bands of polyethylene are expected in the reflection infrared
478 spectra of all the samples analysed (CF-W, ACF-W, CG and WG). IR spectra obtained
479 are shown in Fig. 2. Note that the characteristic bands of polyethylene are given by IG
480 spectrum used for reference. In this sense, two polyethylene peaks can be observed at
481 approximately 2915 and 2850 cm^{-1} (fig. 2a), assigned to asymmetric and symmetric
482 stretching vibrations of C-H bonds in methylene groups (Heydariaraghi et al., 2016). In
483 addition, a strong absorption band at 1470 cm^{-1} and a less strong peak at 720 cm^{-1} (Fig.
484 2b) due to the bending vibrations of C-H bonds in polyethylene are also an indication of

485 the presence of methylene as a functional group (Heydariaraghi et al., 2016). By
486 comparing IG spectrum with the rest of samples, it can be confirmed the presence of
487 polyethylene in all plastic waste samples. However, the presence of polypropylene is
488 also observed in all samples, because there is an additional peak at 1375 cm^{-1} assigned
489 to symmetrical bending vibrations of C-H bonds in methyl groups (Fig. 2b)
490 (Heydariaraghi et al., 2016; Marshall et al., 2005). It is important to note that the
491 intensity of polyethylene bands related to methylene groups is much stronger than that
492 of the peaks corresponding to methyl groups. This finding confirms that plastic waste
493 samples are mainly made up of polyethylene with minority presence of polypropylene.
494 The observed changes in peak intensity imply some changes in relation to the phase or
495 crystallinity of the polymers (polyethylene and/or polypropylene). This observation has
496 also been corroborated by DSC results (Fig. 3). Regarding the pretreatment influence,
497 Fig. 2 reveals the presence of undesired materials (e.g. paper/cardboard, PET, etc.) in
498 untreated samples (CF-W and ACF-W), because characteristic absorption bands,
499 assigned to lignocellulosic materials and PET, have been detected in the FT-IR spectra
500 of CF-W and ACF-W, whereas these additional bands are negligible in the spectra of
501 pretreated materials (CG and WG) and polyethylene (IG). In this regard, it can be
502 observed that CF-W and ACF-W presents two broad bands in the wavenumber ranges
503 of $3600\text{-}3000\text{ cm}^{-1}$ and $1200\text{-}900\text{ cm}^{-1}$, which are characteristics for stretching
504 vibrations of O-H and C-O bonds in lignocellulosic materials (Hospodarova et al.,
505 2018). The presence of PET may also contribute to those observed peaks in line with
506 characteristic bands of PET polymer reported by Pereira et al. (2017). In addition, the
507 presence of this type of polymer has also been detected by DSC (Fig. 3) for ACF-W
508 (automated sorting). The intensity of characteristics bands of undesired materials is
509 higher in plastic waste recovered from automated sorting (ACF-W) than manual sorting

510 (CF-W). Considering this fact, along with results from ultimate analysis and TGA/DTG
511 analysis, it can be concluded that ACF-W presents a higher PET contamination than
512 CF-W. This fact should be taken into account by chemical recycling technology users
513 when they select the feedstock origin based on the requirements of each technology.
514 As indicated in section 3.2, a great variety of chemical compounds are used in
515 polymers, such as antioxidants (e.g. phenols, amines, thioester, etc.), photo-stabilizers
516 (hydroxyaromatic compounds), heat stabilizers (metallic salts, organometallic
517 compounds, etc.), flame retardants (aluminium trihydroxide and magnesium hydroxide,
518 halogenated compounds, phosphorous-based compounds, etc.) and pigments. According
519 to this fact, the presence of characteristic bands due to the stretching vibrations of C-O,
520 O-H, N-H, C=O, C=C, C=N, organometallic and halogenated bonds (Larkin, 2011) is
521 also detected (Fig. 2b) in all samples. For example, the presence of absorption peaks at
522 1170 and 1260 cm^{-1} , assigned to C-O stretching vibrations, are consistent with the
523 presence of phenolic compounds used as polymer additives, mainly primary
524 antioxidants. Characteristic band assigned to C=O stretching vibrations of carboxylic
525 acid group at 1730 cm^{-1} was also detected in all samples, which may be attributed to the
526 presence of polymer additives or the photo-thermal oxidative phenomena typical of
527 polymeric materials occurring at one or all of the manufacturing, processing and end-
528 use stages (Gardette et al., 2013). In addition, the broad absorbance band in the range of
529 1430 cm^{-1} due to the antisymmetric stretching vibration of C-O as well as the peak
530 appeared at 875 cm^{-1} due to the plane of bending vibration of C-O may confirm the
531 presence of calcite (Harris et al., 2015; Sağm et al., 2012), the most used polymer
532 additive for improving mechanical properties of polyethylene. According to literature
533 (Marshall et al., 2005; Öztas and Yürüm, 2000), the overlapped peaks observed in the
534 region of 1200-900 cm^{-1} may also be assigned to the presence of silica (Si-O stretching

535 vibrations at 1100-1000 cm^{-1}). These observations are also supported by the results of
536 metal determination (Table 3).

537

538 FT-IR results related to polymer composition are confirmed by DSC analysis, in which
539 the values of endothermic peak maximum indicate the melting point and type of
540 polymer. The ratio of peak areas is an indication of the polymeric composition. Fig. 3
541 shows the DSC scans obtained from the second heating scanning of the post-consumer
542 plastic film waste CF-W (manual sorting), ACF-W (automated sorting), pretreated
543 samples (CG and WG, respectively) and industrial recycled film granules (IG; reference
544 material for polyethylene), showing a double peak with maxima at around 110 and 122
545 $^{\circ}\text{C}$ for all the samples. This is due to the molecular weight distribution in polyethylene.
546 According to literature ([Liu et al., 2002](#)), the former temperature peak corresponds to
547 LDPE (melting peak ranging from 105-115 $^{\circ}\text{C}$) while the latter one to LLDPE (melting
548 peak ranging from 115-128 $^{\circ}\text{C}$). These values are shifted to lower temperatures as the
549 crystallinity degree is decreased. It is important to note that the higher the density is, the
550 higher the peak temperature and the larger the melting point are. The values of total
551 melting heat associated with these peaks are 97.3 J/g (CF-W), 58.7 J/g (ACF-W), 108.7
552 J/g (CG), 115.4 J/g (WG) and 105.1 J/g (IG), which correspond to 33.2, 20.0, 37.1, 39.4
553 and 35.9 % crystallinity, respectively, based on the reported theoretical value of 293 J/g
554 for 100 % crystalline polyethylene ([Wunderlich, 1990](#)). By comparing the ratio of peak
555 areas between LDPE and LLDPE, it can be concluded that samples obtained from
556 colour film mainly comprise LLDPE, whereas the amount of LDPE is higher in white
557 film samples. An additional peak is observed at around 160-165 $^{\circ}\text{C}$. This peak is
558 ascribed to the presence of polypropylene, which appears to be higher in colour film
559 waste (see comparative DSC scans for CG and WG in [supporting information](#)). ACF-W
560 (automated sorting) also presents a peak at 240 $^{\circ}\text{C}$, which is assigned to PET (see

561 specific DSC scan for ACF-W in [supporting information](#)). It is important to indicate
562 that the presence of PET can only be corroborated from DSC results for ACF-W.

563

564 3.5. *Rheological study*

565 Fig. 4 plots the viscosity curves obtained at different temperatures of the pretreated
566 materials (CG and WG), revealing that temperature and shear rate are critical variables.
567 It is also found that viscosity is shear rate dependent. Both materials exhibit a decreased
568 viscosity with increasing shear rate when the stress is large enough (especially at values
569 greater than 0.1 s^{-1}), showing an abrupt transformation in flow regimes over a relatively
570 narrow range of stress ($\sim 0.1\text{-}1 \text{ s}^{-1}$). This fact is indicative of a shear-thinning non-
571 Newtonian fluid ([Xie and Jin, 2016](#)). Viscosity also decreases significantly as the
572 temperature of the molten polymer increases (see [supporting information](#)). The Cross
573 rheology equation has been widely used to investigate non-Newtonian behaviours ([Xie
574 and Jin, 2016](#)). Considering this, Fig. 4 shows the comparison between numerical
575 (Cross model) and experimental results at different temperatures. Note that the fitting
576 using Cross model faithfully reproduces the experimental data. Cross model parameters
577 are listed in [supporting information](#). In flow curves, in which high-shear rates could not
578 be experimentally reached, viscosity values were modelled considering a shear-thinning
579 behaviour similar to that of the same material at the minimum temperature tested (260
580 °C). On the basis of the analysis of Fig. 4, it can be concluded that viscosity values at a
581 given shear rate and temperature are higher for CG (colour film granules) than for WG
582 (white film granules). This may be an indication of a higher LLDPE content in CG. As
583 previously reported ([Abraham et al., 1992](#); [Brydson, 1999](#); [Liu et al., 2002](#)), the greater
584 the branching of polyethylene is, the lower the viscosity is.

585

586 It is well known that viscosity curves are an important tool for the design of processes
587 in which non-Newtonian fluids take place. In this case, the results of the rheological
588 study could be particularly important keeping in mind that the materials consist of
589 blends of recycled plastics (Ponz, 2009).

590

591 3.6. PVT diagram

592 Fig. 5 shows the PVT diagrams of the pretreated materials (CG and WG), describing the
593 specific volume as a function of pressure and temperature. Specific volume data enables
594 to gain better understanding about unitary steps in industrial processing of polymers or
595 as an input for constitutive models used in process simulation software. This justifies
596 the need of accurately determining the specific volume at conditions comparable to
597 industrial processing conditions. As can be observed in Figure 5, specific volume
598 increases when increasing temperature and decreasing pressure. For example, the
599 specific volume for WG (white film granules) at 7 bar is observed to increase from 1.37
600 $\text{cm}^3 \cdot \text{g}^{-1}$ at 200 °C to 1.60 $\text{cm}^3 \cdot \text{g}^{-1}$ when temperature is increased up to 400 °C. An
601 increase in pressure for WG from 7 to 200 bar at 200 °C results in a decrease in specific
602 volume from 1.37 to 1.35 $\text{cm}^3 \cdot \text{g}^{-1}$. It is worth to note that the influence of pressure on
603 specific volume is less important than temperature. From the results shown in Figure 5,
604 it can also be concluded that specific volume at a given temperature and pressure is
605 significantly higher for WG (white film granules) than CG (colour film granules). The
606 higher density of CG compared to WG confirms the greater presence of LLDPE in CG,
607 since this type of polymer contains lower amounts of long-chain branching than LDPE,

608 as well as a minor average molecular weight (Liu et al., 2002). This finding is also in
609 agreement with rheological and DSC results, showing a higher LLDPE content in CG
610 than in WG. There is also a thermal transition in both types of materials, corresponding
611 to the change of state between solid and melted. The type of thermal transition observed
612 in both samples reveals that they are semi-crystalline polymers because the structural
613 continuity is maintained above the glass transition temperature (Wang, 2012). IKV
614 model parameters for CG and WG are summarized in [supporting information](#).

615

616 3.7. Determination of specific heat capacity

617 Specific heat capacity was measured by using MDSC (Modulated Differential Scanning
618 Calorimetry) for CG (colour film granules) and WG (white film granules) samples. Fig.
619 6 shows how specific heat capacity (C_p) changes as a function of temperature. The
620 endothermic peaks observed at temperatures near 120 (WG) – 125 °C (CG) indicate the
621 glass transition due to polymer melting. As can be observed, the values of the specific
622 heat capacity for WG are significantly higher than CG prior to melting point. The
623 specific heat capacity reaches up to approximately $4.2 \text{ J}\cdot\text{g}^{-1}\cdot\text{°C}^{-1}$ for WG, while this
624 value is $3.3 \text{ J}\cdot\text{g}^{-1}\cdot\text{°C}^{-1}$ for CG. These observations are indicative of a higher
625 LDPE/LLDPE ratio in WG compared to CG. These results are consistent with DSC,
626 rheological and PVT diagram data. Once the temperature is increased above the melting
627 region, the value of the specific heat capacity is remarkably lower and no substantial
628 differences are observed between both materials. The data obtained by DSC technique
629 together with determination of specific heat capacity are particularly important in
630 processes involving phase changes where heat transfer and temperatures play an
631 essential role. This is the case in the most of chemical recycling processes.

632 3.8. *Determination of halogen and sulphur contents*

633 Halogen and sulphur containing compounds are often added as plasticizers, flame
634 retardant and heat stabilizers. Due to their serious impact, it is important to know the
635 content of halogens and sulphur when polymers are recycled or used as a raw material
636 in thermochemical technologies. The pretreated materials (CG and WG) were found to
637 contain very little halogens and sulphur. Sulphur was found to be in a low concentration
638 (~ 85 ppm) in colour and white film granules (CG and WG, respectively). The halogen
639 content expressed as chlorine is slightly higher in WG (1095 ppm) compared to CG
640 (928 ppm).

641

642 **4. Conclusions**

643 Detailed characterization of different post-consumer plastic film waste samples coming
644 from mixed MSW in Spain and recovered by manual (CF: colour film waste; WF: white
645 film waste) and automated sorting (ACF: Colour film waste) samples, provided critical
646 information for Life Cycle Assessment (LCA) and implementing innovations in
647 chemical recycling technologies (i.e. pyrolysis) to enable the transformation of plastic
648 waste into valuable resources. The results were contrasted with those obtained for
649 pretreated plastic film waste (CG – colour film granules and WG – white film granules)
650 and industrial recycled film granules (IG; as a reference material for packaging film). It
651 was found that the type of sorting plays an important role on the plastic waste quality
652 and composition, strongly affecting the presence of additives and contaminants
653 (quantity and type). It can also be concluded that the pretreatment may be needed for the
654 successful commercial application of novel cost and energy-efficient alternatives of
655 current chemical recycling, especially in the case of colour plastic film waste
656 management. However, white plastic film waste stream exhibited a greater potential to

657 be used directly in chemical recycling process, since its characteristics were observed to
658 be very close to those observed for industrial recycled film granules (IG). Despite this,
659 it is important to note that even white plastic film may require a pretreatment step
660 depending on the final application. For each recycling technology, a specific
661 pretreatment should be designed based on the process requirements. Finally, no clear
662 influence of seasonality on plastic waste quality recovered by manual sorting was
663 observed, so characteristics of this plastic waste stream are always kept constant. This is
664 a positive issue to improve and optimize the design of pretreatment processes,
665 guaranteeing its use in fastly-evolving recycling technologies.

666

667 **Acknowledgements**

668 The authors acknowledge the financial support of the Centre for the Development of
669 Industrial Technology [grant number IDI – 20181081] and the Ministerio de Ciencia,
670 Innovación y Universidades (Spain) [grant number DI – 16 – 08700].

671

672 **References**

673 **Abraham, D., George, K.E., Francis, D.J., 1992.** Melt viscosity and elasticity of low
674 density and linear low density polyethylene blends. *Int. J. Polym. Mater. Po.* 18, 197-

675 211. <https://doi.org/10.1080/00914039208029321>

676 **Achilias, D.S., Roupakias, C., Megalokonomos, P., Lappas, A.A., Antonakou, V.,**
677 **2007.** Chemical recycling of plastic wastes made from polyethylene (LDPE and HDPE)
678 and polypropylene (PP). *J Hazard. Mater.* 149, 536–542.

679 <https://doi.org/10.1016/j.jhazmat.2007.06.076>

680 **AENOR (Asociación Española de Normalización y Certificación), 2005.** UNE
681 53087 – 2:2005 Plastics and rubber. Determination of chlorine content. Part 2. Method
682 of coulombimetry.

683 **Al-Salem, S. M., 2019.** Feedstock and optimal operation for plastics to fuel conversion
684 in pyrolysis, in: Al-Salem, S. M. (Ed.), *Plastics to Energy: Fuel, Chemicals, and*
685 *Sustainability Implications*. William Andrew Publishing, pp. 117-146.
686 <https://doi.org/10.1016/B978-0-12-813140-4.00005-4>

687 **Alvarenga, L.M., Xavier, T.P., Barrozo, M.A.S., Bacelos, M.S., Lira, T.S., 2016.**
688 Determination of activation energy of pyrolysis of carton packaging wastes and its pure
689 components using thermogravimetry. *Waste Manage.* 53, 68-75.
690 <https://doi.org/10.1016/j.wasman.2016.04.015>

691 **Ambrogi, V., Carfagna, C., Cerruti, P., Marturano, V., 2017.** Additives in polymers,
692 in: Jasso-Gatinel, C.F., Kenny (Eds.), *Modification of polymer properties*. William
693 Andrew Publishing, pp. 87-108. <https://doi.org/10.1016/B978-0-323-44353-1.00004-X>

694 **Angyal, A., Miskolczi, N., Bartha, L., 2007.** Petrochemical feedstock by thermal
695 cracking of plastic waste. *J. Anal. Appl. Pyrol.* 79, 409–414.
696 <https://doi.org/10.1016/j.jaap.2006.12.031>

697 **Argyle, M.D., Bartholomew, C.H., 2015.** Heterogeneous catalyst deactivation and
698 regeneration: A review. *Catalysts.* 5, 145-269. <http://doi.org/10.3390/catal5010145>

699 **ASTM International, 2017.** E2550 – 17 Standard test method for thermal stability by
700 thermogravimetry. <http://doi.org/10.1520/E2550-17>

701 **Balakrishnan, P., Thomas, M.S., Pothen, L.A., Thomas, S., Sreekala, M.S., 2014.**
702 Polymer films for packaging, in: Kobayashi, S., Müllen, K. (Eds.), *Encyclopedia of*
703 *Polymeric Nanomaterials*. Springer, Berlin, Heidelberg, pp. 1-8.
704 http://doi.org/10.1007/978-3-642-36199-9_406-1

705 **BASF, 2018.** BASF makes products with chemically recycled plastics for first time.
706 https://www.coatingsworld.com/contents/view_breaking-news/2018-12-13/basf-makes-
707 [products-with-chemically-recycled-plastics-for-first-time/](https://www.coatingsworld.com/contents/view_breaking-news/2018-12-13/basf-makes-products-with-chemically-recycled-plastics-for-first-time/) (accessed 15 April 2020).

708 **Bisinella, V., Götze, R., Conradsen, K., Damgaard, A., Christensen, T., Astrup,**
709 **T.F., 2017.** Importance of waste composition for Life Cycle Assessment of waste
710 management solutions. *Journal of Cleaner Production*, 164, pp. 1180-1191.
711 <https://doi.org/10.1016/j.jclepro.2017.07.013>

712 **Boyard, N., Delaunay, D., 2016.** Experimental determination and modeling of
713 thermophysical properties, in: Boyard, N. (Ed.), *Heat Transfer in Polymer Composite*
714 *Materials: Forming Processes*. John Wiley & Sons, Inc., London, Great Britain, pp. 29 –
715 76. <https://doi.org/10.1002/9781119116288.ch2>

716 **British Plastics Federation.** <https://www.bpf.co.uk/packaging/Default.aspx> (accessed
717 20 September 2019).

718 **Brydson, J.A., 1999.** Relation of structure to thermal and mechanical properties, in:
719 Brydson, J.A. (Ed.), *Plastics Materials (Seven Edition)*. Butterworth-Heinemann, pp.
720 59-75. <https://doi.org/10.1016/B978-075064132-6/50045-0>

721 **CEN (European Committee for Standardization), 2006.** CEN/TR 15310-3:2006
722 *Characterization of waste – Sampling of waste materials – Part 3: Guidance on*
723 *procedures for sub – sampling in the field*. Work Item Number: 00292018.

724 **CEN (European Committee for Standardization), 2011a.** EN 15407:2011 *Solid*
725 *recovered fuels – Methods for the determination of carbon (C), hydrogen (H) and*
726 *nitrogen (N) content*. Work Item Number: 00343057.

727 **CEN (European Committee for Standardization), 2011b.** EN 15414 – 3:2011 *Solid*
728 *recovered fuels – Determination of moisture content using the oven dry method – Part*
729 *3: Moisture in general analysis sample*. Work Item Number: 00343055.

730 **CEN (European Committee for Standardization), 2011c.** EN 15402:2011 Solid
731 recovered fuels – Determination of the content of volatile matter. Work Item Number:
732 00343048.

733 **CEN (European Committee for Standardization), 2011d.** EN 15403:2011 Solid
734 recovered fuels – Determination of ash content. Work Item Number: 00343049.

735 **CEN (European Committee for Standardization), 2011e.** EN 15400:2011 Solid
736 recovered fuel – Determination of calorific value. Work Item Number: 00343046.

737 **CEN (European Committee for Standardization), 2011f.** EN 15407:2011 Solid
738 recovered fuel – Methods for the determination of carbon (C), hydrogen (H) and
739 nitrogen (N) content. Work Item Number: 00343057.

740 **CEN (European Committee for Standardization), 2011g.** EN 15410:2012 Solid
741 recovered fuel – Methods for the determination of the content of major elements (Al,
742 Ca, Fe, K, Mg, Na, P, Si, Ti). Work Item Number: 00343059.

743 **CEN (European Committee for Standardization), 2018.** EN ISO 11357-3:2018
744 Plastics – Differential scanning calorimetry (DSC) – Part 3: Determination of
745 temperature and enthalpy of melting and crystallization (ISO 11357 – 3:2018). Work
746 Item Number: 00249987.

747 **Circular economy strategy, 2019.** European commission, Environment.
748 http://ec.europa.eu/environment/circular-economy/index_en.htm (accessed 29 May
749 2019).

750 **Cross, M.M., 1965.** Rheology of non-Newtonian fluids: A new flow equation for
751 pseudoplastic systems. J. Colloid Sci. 20 (5), 417-437. [https://doi.org/10.1016/0095-](https://doi.org/10.1016/0095-8522(65)90022-X)
752 [8522\(65\)90022-X](https://doi.org/10.1016/0095-8522(65)90022-X)

753 **Czajczyńska, D., Anguilano, L., Ghazal, H., Krzyżyńska, R., Reynolds, A.J.,**
754 **Spencer, N., Jouhara, H., 2017.** Potential of pyrolysis processes in the waste

755 management sector. *Therm. Sci. Eng. Prog.* 3, 171-197.
756 <http://doi.org/10.1016/j.tsep.2017.06.003>

757 **Dahlbo, H., Poliakova, V., Mylläri, V., Sahimaa, O., Anderson, R., 2018.** Recycling
758 potential of post-consumer plastic packaging waste in Finland. *Waste Manage.* 71, 52-
759 61. <https://doi.org/10.1016/j.wasman.2017.10.033>

760 **Diaz-Silvarrey, L.S. Phan, A.N., 2016.** Kinetic study of municipal plastic waste. *Int. J.*
761 *Hydrogen Energy.* 41, 16352-16364. <http://doi.org/10.1016/j.ijhydene.2016.05.202>

762 **Dwivedi, P., Mishra, P.K., Mondal, M.K., Srivastava, N., 2019.** Non-biodegradable
763 polymeric waste pyrolysis for energy recovery. *Heliyon.* 5, e02198.
764 <https://doi.org/10.1016/j.heliyon.2019.e02198>

765 **Dymond, J.H., Malhotra, R., 1988.** The Tait equation: 100 years on. *Int. J.*
766 *Thermophys.* 9: 941 – 951. <https://doi.org/10.1007/BF01133262>

767 **Ellen MacArthur Foundation, 2016.** The new plastics economy: Rethinking the future
768 of plastics.
769 [https://www.ellenmacarthurfoundation.org/assets/downloads/EllenMacArthurFoundatio](https://www.ellenmacarthurfoundation.org/assets/downloads/EllenMacArthurFoundation_TheNewPlasticsEconomy_Pages.pdf)
770 [n_TheNewPlasticsEconomy_Pages.pdf](https://www.ellenmacarthurfoundation.org/assets/downloads/EllenMacArthurFoundation_TheNewPlasticsEconomy_Pages.pdf) (accessed 29 May 2019).

771 **EU, 2008.** Directive 2008/98/EC of the European Parliament and of the Council of 19
772 November 2008 on waste and repealing certain directives. [https://eur-](https://eur-lex.europa.eu/eli/dir/2008/98/oj)
773 [lex.europa.eu/eli/dir/2008/98/oj](https://eur-lex.europa.eu/eli/dir/2008/98/oj) (accessed 29 May 2019).

774 **EU, 2018.** Directive (EU) 2018/850 of the European Parliament and of the Council of
775 30 May 2018 amending Directive 1999/31/EC on the landfill of waste (Text with EEA
776 relevance) [https://eur-lex.europa.eu/legal-](https://eur-lex.europa.eu/legal-content/es/TXT/?uri=CELEX%3A32018L0850)
777 [content/es/TXT/?uri=CELEX%3A32018L0850](https://eur-lex.europa.eu/legal-content/es/TXT/?uri=CELEX%3A32018L0850) (accessed 29 May 2019).

778 **European Parliamentary Research Service Blog, 2017.** Plastics in a circular
779 economy: opportunities and challenges. [https://epthinktank.eu/2017/05/18/plastics-in-a-](https://epthinktank.eu/2017/05/18/plastics-in-a-circular-economy-opportunities-and-challenges/)
780 [circular-economy-opportunities-and-challenges/](https://epthinktank.eu/2017/05/18/plastics-in-a-circular-economy-opportunities-and-challenges/) (accessed 29 May 2019).

781 **Faraca, G., Astrup, T., 2019.** Plastic waste from recycling centres: Characterization
782 and evaluation of plastic recyclability. *Waste Manage.* 95, 388 – 398.
783 <https://doi.org/10.1016/j.wasman.2019.06.038>

784 **Gardette, M., Thérias, S., Gardette, J.L., Janecska, T., Földes, E., Pukánszky, B.,**
785 **2013.** Photo- and thermal-oxidation of polyethylene: Comparison of mechanisms and
786 influence of unsaturation content. *Polym. Degrad. Stabil.* 98, 2383-2390.
787 <http://dx.doi.org/10.1016/j.polymdegradstab.2013.07.017>

788 **Gorghiu, L.M., Jipa, S., Zaharescu, T., Setnescu, R., Mihalcea, I., 2004.** The effect
789 of metals on thermal degradation of polyethylenes. *Polym. Degrad. Stabil.* 84, 7-11.
790 [https://doi.org/10.1016/S0141-3910\(03\)00265-9](https://doi.org/10.1016/S0141-3910(03)00265-9)

791 **Harris, J., Mey, I., Hajir, M., Mondeshki, M., Wolf, S.E., 2015.** Pseudomorphic
792 transformation of amorphous calcium carbonate films follows spherulitic growth
793 mechanisms and can give rise to crystal lattice tilting. *Crys. Eng. Comm.* 17, 6831-
794 6837. <https://doi.org/10.1039/c5ce00441a>

795 **Heikkinen, J.M., Hordijk, J.C., de Jong, W., Spliethoff, H., 2004.** Thermogravimetry
796 as a tool to classify waste components to be used for energy generation. *J. Anal. Appl.*
797 *Pyrol.* 71, 883-900. <https://doi.org/10.1016/j.jaap.2003.12.001>

798 **Hestin, M., Faninger, T., Milios, L., 2015.** Increased EU plastics recycling targets:
799 Environmental, economic and social impact assessment.
800 [https://www.plasticsrecyclers.eu/sites/default/files/BIO_Deloitte_PRE_Plastics%20Rec-](https://www.plasticsrecyclers.eu/sites/default/files/BIO_Deloitte_PRE_Plastics%20Recycling%20Impact_Assesment_Final%20Report.pdf)
801 [ycling%20Impact_Assesment_Final%20Report.pdf](https://www.plasticsrecyclers.eu/sites/default/files/BIO_Deloitte_PRE_Plastics%20Recycling%20Impact_Assesment_Final%20Report.pdf) (accessed 29 May 2019).

802 **Heydariaraghi, M., Ghorbanian, S., Hallajisani, A., Salehpour, A., 2016.** Fuel
803 properties of the oils produced from the pyrolysis of commonly-used polymers: Effect
804 of fractionating column. *J. Anal. Appl. Pyrol.* 121, 307-317.
805 <https://doi.org/10.1016/j.jaap.2016.08.010>

806 **Horodytska, O., Valdés, F.J., Fullana, A., 2018.** Plastic flexible films waste
807 management. A state of art review. *Waste Manage.* 77, 413-425.
808 <https://doi.org/10.1016/j.wasman.2018.04.023>

809 **Hospodarova, V., Singovszka, E., Stevulova, N., 2018.** Characterization of cellulosic
810 fibers by FTIR spectroscopy for their further implementation to building materials. *Am.*
811 *J. Analyt. Chem.* 9, 303-310. <https://doi.org/10.4236/ajac.2018.96023>

812 **Hubbe, M.A., Gill, R.A., 2016.** Fillers for papermaking: A review of their properties,
813 usage practices, and their mechanistic role. *BioRes.* 11, 2886-2963.
814 <https://doi.org/10.15376/biores.11.1.2886-2963>

815 **Hujuri, U., Ghoshal, A.K., Gumma, S., 2008.** Modeling pyrolysis kinetics of plastic
816 mixtures. *Polym. Degrad. Stab.* 93, 1832-1837.
817 <https://doi.org/10.1016/j.polymdegradstab.2008.07.006>

818 **Khoo, H.H., 2019.** LCA of plastic waste recovery into recycled materials, energy and
819 fuels in Singapore. *Resour. Conserv. Recy.* 145, 67-77.
820 <https://doi.org/10.1016/j.resconrec.2019.02.010>

821 **Kumar, S., Singh, R.K., 2011.** Recovery of hydrocarbon liquid from waste high
822 density polyethylene by thermal pyrolysis. *Braz. J. Chem. Eng.* 28, 659-667.
823 <http://doi.org/10.1590/S0104-66322011000400011>

824 **Kunwar, B., Cheng, H.N., Chandrashekar, S.R., Sharma, B.K., 2016.** Plastics to
825 fuel: A review. *Renew. Sustain Energy Rev.* 54, 421-428.
826 <http://doi.org/10.1016/j.rser.2015.10.015>

827 **Lafia-Araga, R.A., Hassan, A., Yahya, R., Rahman, N.A., Hornsby, P.R.,**
828 **Heidarian, J., 2012.** Thermal and mechanical properties of treated and untreated Red
829 Balau (*Shorea dipterocarpaceae*)/LDPE composites. *J. Reinf. Plast. Compos.* 31, 215-
830 224. <https://doi.org/10.1177/0731684411433913>

831 **Larkin, P., 2011.** Chapter 8 – Illustrated IR and Raman spectra demonstrating
832 important functional groups, in: Larkin, P. (Ed.), *Infrared and Raman Spectroscopy.*
833 Elsevier, pp. 135-176. <https://doi.org/10.1016/B978-0-12-386984-5.10008-4>

834 **Liu, C., Wang, J., He, J., 2002.** Rheological and thermal properties of m-LLDPE
835 blends with m-HDPE and LDPE. *Polymer.* 43, 3811-3818.
836 [https://doi.org/10.1016/S0032-3861\(02\)00201-X](https://doi.org/10.1016/S0032-3861(02)00201-X)

837 **Lopez, G., Artetxe, M., Amutio, M., Bilbao, J., Olazar, M., 2017.** Thermochemical
838 routes for the valorization of waste polyolefinic plastics to produce fuels and chemicals.
839 A review. *Renew. Sustain. Energy. Rev.* 73, 346-368.
840 <http://doi.org/10.1016/j.rser.2017.01.142>

841 **Mastellone, M. L., 2019.** A feasibility assessment of an integrated plastic waste system
842 adopting mechanical and thermochemical conversion processes. *Resour. Conservation.*
843 *Recycl. : X.* 9, 100017. <https://doi.org/10.1016/j.rcrx.2019.100017>

844 **Marshall, C. P., Kannangara, G. S. K., Alvarez, R., Wilson, M. A., 2005.**
845 Characterisation of insoluble charcoal in Weipa bauxite. *Carbon.* 43, 1279-1285.
846 <http://doi.org/10.1016/j.carbon.2004.12.024>

847 **NESTE, 2018.** Neste aiming to use waste plastic as a raw material for fuels and
848 plastics. [https://www.neste.com/releases-and-news/circular-economy/neste-aiming-use-](https://www.neste.com/releases-and-news/circular-economy/neste-aiming-use-waste-plastic-raw-material-fuels-and-plastics)
849 [waste-plastic-raw-material-fuels-and-plastics](https://www.neste.com/releases-and-news/circular-economy/neste-aiming-use-waste-plastic-raw-material-fuels-and-plastics) (accessed 15 April 2020).

850 **Oasmaa, A., Qureshi, M., S., Pihkola, H., Deviatkin, I., Mannila, J., Tenhunen, A.,**
851 **Minkkinen, H., Pohjakallio, M., Laine-Ylijoki, J., 2020.** Pyrolysis of plastic waste:

852 Opportunities and challenges. *J. Anal. Appl. Pyrol.* In Press, 104804.
853 <https://doi.org/10.1016/j.jaap.2020.104804>

854 **Ojeda, T., 2013.** Polymer degradation, in: IntechOpen, *Polymers and the Environment*.
855 <http://doi.org/10.5772/51057>

856 **Öztaş, N. A., Yürüm, Y., 2000.** Pyrolysis of Turkish Zonguldak bituminous coal. Part
857 1. Effect of mineral matter. *Fuel.* 79, 1221-1227.
858 [http://doi.org/10.1016/S0016-2361\(99\)00255-0](http://doi.org/10.1016/S0016-2361(99)00255-0)

859 **Panda, A.K., Singh, R.K., Mishra, D.K., 2010.** Thermolysis of waste plastics to liquid
860 fuel: A suitable method for plastic waste management and manufacture of value added
861 products: A world prospective. *Renew. Sustain Energy Rev.* 14, 233–48.
862 <https://doi.org/10.1016/j.rser.2009.07.005>

863 **Park, K.B., Jeong, Y.S., Guzelciftci, B., Kim, J.S., 2019.** Characteristics of a new type
864 continuous two-stage pyrolysis of waste polyethylene. *Energy.* 166, 343-351.
865 <https://doi.org/10.1016/j.energy.2018.10.078>

866 **Pereira, A.P.S., Silva, M.H.P., Júnior, E.P.L., Paula, A.S., Tommasini, F.J., 2017.**
867 Processing and characterization of PET composites reinforced with geopolymer
868 concrete waste. *Mater. Res.* 20, 411-420. [http://doi.org/10.1590/1980-5373-mr-2017-](http://doi.org/10.1590/1980-5373-mr-2017-0734)
869 [0734](http://doi.org/10.1590/1980-5373-mr-2017-0734)

870 **Pinto, F., Costa, P., Gulyurtlu, I., Cabrita, I., 1999.** Pyrolysis of plastic wastes. 1.
871 Effect of plastic waste composition on product yield. *J. Anal. Appl. Pyrol.* 51, 39 – 55.
872 [https://doi.org/10.1016/S0165-2370\(99\)00007-8](https://doi.org/10.1016/S0165-2370(99)00007-8)

873 **Plastics Europe, 2018.** *Plastics –the Facts 2018.* An analysis of European plastics
874 production, demand and waste data.
875 <https://www.plasticseurope.org/en/resources/publications/619-plastics-facts-2018>
876 (accessed 29 May 2019).

877 **Plastics Europe, 2019a.** Plastics –the Facts 2019. An analysis of European plastics
878 production, demand and waste data.
879 <https://www.plasticseurope.org/en/resources/publications/1804-plastics-facts-2019>
880 (accessed 20 January 2020).

881 **Plastics Europe, 2019b.** The circular economy for plastics. A European overview.
882 [https://www.plasticseurope.org/en/resources/publications/1899-circular-economy-](https://www.plasticseurope.org/en/resources/publications/1899-circular-economy-plastics-european-overview)
883 [plastics-european-overview](https://www.plasticseurope.org/en/resources/publications/1899-circular-economy-plastics-european-overview) (accessed 20 January 2020).

884 **Ponz, L., 2009.** Metodología para la caracterización reológica de materiales
885 termoplásticos en condiciones no convencionales para su aplicación a herramientas de
886 simulación, Aplicación a un PEHD reciclado, Thesis (Ph.D), Universidad de Zaragoza.

887 **Ragaert, K., Delva, L., Van Geem, K., 2017.** Mechanical and chemical recycling of
888 solid plastic waste. Waste Manage. 69, 24-58.
889 <https://doi.org/10.1016/j.wasman.2017.07.044>

890 **REPSOL, 2020.** We obtain the ISCC Plus certification for all our petrochemical
891 complexes. [https://www.repsol.com/en/products-and-services/chemicals/news/we-](https://www.repsol.com/en/products-and-services/chemicals/news/we-obtain-the-iscc-plus-certification-for-all-our-petrochemical-complexes/index.cshtml)
892 [obtain-the-iscc-plus-certification-for-all-our-petrochemical-complexes/index.cshtml](https://www.repsol.com/en/products-and-services/chemicals/news/we-obtain-the-iscc-plus-certification-for-all-our-petrochemical-complexes/index.cshtml)
893 (accessed 15 April 2020)

894 **Ruj, B., Pandey, V., Jash, P., Srivastava, V.K., 2015.** Sorting of plastic waste for
895 effective recycling. Int. J. App. Sci. Eng. Res. 4 (4), pp. 564-571.

896 **Sağm, E.U., Böke, H., Aras, N., Yalçm, Ş., 2012.** Determination of CaCO₃ and SiO₂
897 content in the binders of historic lime mortars. Mater. Struct. 45, 841-849.
898 <https://doi.org/10.1617/s11527-011-9802-1>

899 **Sarker, M., Rashid, M.M., 2013.** Mixture of LDPE, PP and PS waste plastics into fuel
900 by thermolysis process. Int. J. Eng. Tech. Res. 1, 1-16.

901 **Scott, R., Granchell, J., 2013.** Analysis of metals content in Thermo Scientific Nalgene
902 HDPE bottles and competitors. Application Note. Thermo Scientific.
903 [https://assets.thermofisher.com/TFS-Assets/LCD/Application-](https://assets.thermofisher.com/TFS-Assets/LCD/Application-Notes/ANLSPMTLHDPEBTL-0713-HDPE-Bottle-Metal.pdf)
904 [Notes/ANLSPMTLHDPEBTL-0713-HDPE-Bottle-Metal.pdf](https://assets.thermofisher.com/TFS-Assets/LCD/Application-Notes/ANLSPMTLHDPEBTL-0713-HDPE-Bottle-Metal.pdf)

905 **Sharuddin, S.D.A., Abnisa, F., Daud, W.M.A.W., Aroua, M.K., 2016.** A review on
906 pyrolysis of plastic wastes. Energy Convers. Manage. 115, 308-326.
907 <http://doi.org/10.1016/j.enconman.2016.02.037>

908 **Singh, R.K., Ruj, Sadhukhan, A.K., Gupta, P., 2019.** Thermal degradation of waste
909 plastics under non-sweeping atmosphere: Part 1. Effect of temperature, product
910 optimization, and degradation mechanism. J. Environ. Manage. 239, 395-406.
911 <https://doi.org/10.1016/j.jenvman.2019.03.067>

912 **Wang, J., 2012.** PVT properties of polymers for injection molding, some critical issues
913 for injection molding, in: J. Wang (Ed.), Some critical issues for injection molding,
914 IntechOpen. <https://doi.org/10.5772/35212>

915 **Wang, C.Q., Wang, H., Fu, J.G., Liu, Y.N., 2015.** Flotation separation of waste
916 plastics for recycling – A review. Waste Manage. 41, 28-38.
917 <https://doi.org/10.1016/j.wasman.2015.03.027>

918 **Waste and Resources Action Programme, 2016.** Collection and sorting of household
919 plastic film packaging.
920 [http://www.wrap.org.uk/sites/files/wrap/MST1445_Plastic_Film_Breifing_Note_final%](http://www.wrap.org.uk/sites/files/wrap/MST1445_Plastic_Film_Breifing_Note_final%20for%20web.pdf)
921 [20for%20web.pdf](http://www.wrap.org.uk/sites/files/wrap/MST1445_Plastic_Film_Breifing_Note_final%20for%20web.pdf) (accessed 20 September 2019).

922 **Wong S.L., Ngadi N., Abdullah T.A.T., Inuwa I.M., 2017.** Current state and future
923 prospects of plastic waste as source of fuel: A review. Renew. Sustain. Energy. Rev. 50,
924 1167–1180. <https://doi.org/10.1016/j.rser.2015.04.063>

925 **Wunderlich, B., 1990.** Appendix – ATHAS table of thermal properties of linear
 926 macromolecules, in: H.B. Jovanovich (Ed.), Thermal Analysis, Academic Press Inc.,
 927 1990, pp. 417-431. <https://doi.org/10.1016/B978-0-12-765605-2.50012-1>
 928 **Xie, J., Jin, Y.C. 2016.** Parameter determination for the Cross rheology equation and its
 929 application to modeling non-Newtonian flows using the WC-MPS method. Eng. Appl.
 930 Comp. Fluid. 10, 111-129. <https://doi.org/10.1080/19942060.2015.1104267>
 931 **Yan, J., Karlsson, A., Zou, Z., Dai, D., Edlund, U., 2020.** Contamination of heavy
 932 metals and metalloids in biomass and waste fuels: Comparative characterization and
 933 trend estimation. Sci. Total Environ. 700, 134382.
 934 <https://doi.org/10.1016/j.scitotenv.2019.134382>

935

936 **Tables and Figures**

937 **Table 1.**

938 Standards and commercial equipment used for analysing chemical composition, heating values, metal and
 939 halogen contents.

Parameter	Standard	Reference	Equipment
<i>Ultimate analysis</i> CHN/S	EN 15407:2011	CEN, 2011a	LECO CHNS628 / (628S module)
<i>Proximate analysis</i> Moisture	EN 15414-3:2011	CEN, 2011b	Memmert UFE550
Volatile matter	EN 15402:2011	CEN, 2011c	Carbolite AAF 11/18
Ash	EN 15403:2011	CEN, 2011d	Carbolite AAF 11/18
Fixed carbon*			
<i>Heating values</i> HHV	EN 15400:2011	CEN, 2011e	Parr 6100
LHV**	EN 15407:2011	CEN, 2011f	
<i>Metal content</i>	EN 15410:2011	CEN, 2011g	Milestone-ETHOS One (microwave digestion) SPECTRO-GENESIS/SOP (ICP-OES)
<i>DSC analysis</i>	EN ISO 11357-3:2018	CEN, 2018	TA Instruments Q200 DSC
<i>Halogen content</i>	EN 53087-2:2005	AENOR, 2005	Mitsubishi TOX-100 analyser

940 *By difference

941 ** By calculation from HHV and hydrogen content

942 **Table 2.**

943 Results of ultimate analysis (wt. %; dry basis), H/C ratio (molar basis), ash (wt. %, dry basis), proximate

944 analysis (wt. %; as received) and heating values (kJ/kg; dry basis).

	Manual Sorting						Autom. sorting	Pretreatment		Industrial
	Colour film	Colour film	Colour film	Colour film	White film	White film	Colour film	Colour film	White film	Recycled film
	winter	spring	summer	autumn	winter	summer	winter	granules	granules	granules
	CF-W	CF-SP	CF-S	CF-A	WF-W	WF-S	ACF-W	CG	WG	IG
<i>Ultimate analysis</i>										
C	72.7	77.4	69.3	71.8	80.9	81.8	70.7	80.4	84.3	82.8
H	12.3	12.6	11.1	11.4	13.8	13.2	11.1	13.5	14.3	13.9
N	2.4	0.4	0.3	0.4	0.1	0.1	0.6	0.1	0.0	0.0
S	0.3	0.1	0.2	0.2	0.2	0.1	0.2	0.1	0.1	0.1
O*	0.6	0.8	6.0	6.1	2.6	0.1	11.8	0.5	0.3	0.2
<i>H/C ratio</i>	2.03	1.95	1.92	1.91	2.05	1.94	1.88	2.01	2.03	2.01
<i>Ash</i>	11.7	8.7	13.1	10.1	2.4	4.7	5.5	5.4	1.0	3.0
<i>Proximate analysis</i>										
Ash	9.8	7.7	11.2	8.8	2.3	4.6	5.0	5.4	1.0	1.0
Moisture content	15.9	11.0	14.8	13.1	3.0	3.0	9.3	0.1	0.1	0.2
Volatile matter	74.2	81.2	73.4	77.2	94.1	92.3	82.4	94.4	98.8	97.5
Fixed carbon	0.1	0.1	0.6	0.9	0.6	0.1	3.3	0.1	0.1	1.3
<i>Heating Values</i>										
HHV	41127	42394	36366	37775	43727	44684	37541	43581	45947	44860
LHV	38519	39718	34080	35430	40885	41863	35262	40801	43167	41996

945 *By difference

946

947

948

949

950

951

952

	Manual Sorting						Autom. sorting	Pretreatment		Industrial
	Colour film	Colour film	Colour film	Colour film	White film	White film	Colour film	Colour film	White film	Recycled film
	winter	spring	summer	autumn	winter	summer	winter	granules	granules	granules
	CF-W	CF-SP	CF-S	CF-A	WF-W	WF-S	ACF-W	CG	WG	IG
Ag	< 0.8	< 0.8	< 0.8	< 0.8	< 0.8	< 0.8	< 0.8	< 0.8	< 0.8	< 0.8
Al	2093	1093	1539	1858	669	543	2340	190	205	571
As	< 10	< 10	< 10	< 10	< 10	< 10	< 10	< 10	< 10	< 10
B	17	< 4	< 4	9	< 4	< 4	< 4	< 4	< 4	< 4
Ba	115	145	102	96	33	17	53	30	8	36
Bi	6	< 0.6	237	< 0.6	< 0.6	115	< 0.6	-	-	< 0.6
Ca	38856	20597	31568	31081	6088	4740	13583	13236	1300	9464
Cd	< 0.3	< 0.3	< 0.3	< 0.3	< 0.3	< 0.3	< 0.3	< 0.3	< 0.3	< 0.3
Cr	14	< 0.8	15	68	22	8	12	8	7	6
Cu	52	38	24	108	40	< 0.3	22	19	4	170
Fe	1352	2378	-	1760	97	-	1848	187	< 10	162
Ga	< 9	15	41	28	< 9	72	< 9	-	-	11
Hg	-	< 0.2	153	< 0.2	< 0.2	93	< 0.2	< 0.2	< 0.2	< 0.1
K	2326	1089	917	1773	520	491	688	< 208	< 208	< 208
Li	< 4	< 4	< 4	5	7	< 4	< 4	< 4	< 4	< 4
Mg	1428	618	824	926	466	< 422	439	< 422	< 422	< 422
Mn	73	32	9	25	11	< 4	11	< 4	10	-
Mo	< 4	< 4	< 4	8	< 4	< 4	< 4	< 4	< 4	-
Na	1697	1223	1317	2481	691	426	1839	< 185	< 185	< 185
Ni	< 4	20	< 4	26	6	< 4	< 4	< 4	< 4	33
P	914	658	1661	550	202	1986	221	13	29	106
Pb	31	236	< 4	429	5	< 4	< 4	19	< 4	16
Sb	< 10	< 10	< 10	29	< 10	< 10	< 10	< 10	< 10	< 10
Se	< 9	< 9	-	29	< 9	-	< 9	-	-	< 9
Si	< 214	356	1622	484	< 214	1024	< 214	< 214	< 214	380
Sn	23	< 0.8	295	14	2	35	6	9	5	< 0.8
Sr	106	24	19	34	12	7	14	9	< 4	< 4
Ti	1796	495	1605	793	45	812	222	< 4	< 4	427
V	< 4	< 4	< 4	< 4	< 4	< 4	< 4	< 4	< 4	-
Zn	399	265	87	201	86	60	139	93	37	< 0.1
Total (%)	5.2	2.9	4.2	4.3	1.9	1.1	2.2	1.5	0.3	1.2

956 **Table 4.**

957 Summary of the TGA/DTG results (Fig. 1) of post-consumer plastic film waste (manual sorting CF-W;

958 automated sorting ACF-W; granules: CG, WG, IG).

	T5 (°C)	T10 (°C)	T50 (°C)	T80 (°C)	Tmax (°C)	Char content at 800 °C (wt. %)
CF-W	226	283	461	518	476	13.5
ACF-W	289	352	465	488	480	8
CG	404	459	483	493	486	3.5
WG	424	442	474	486	477	-
IG	451	462	482	491	485	3.5

959

960

961

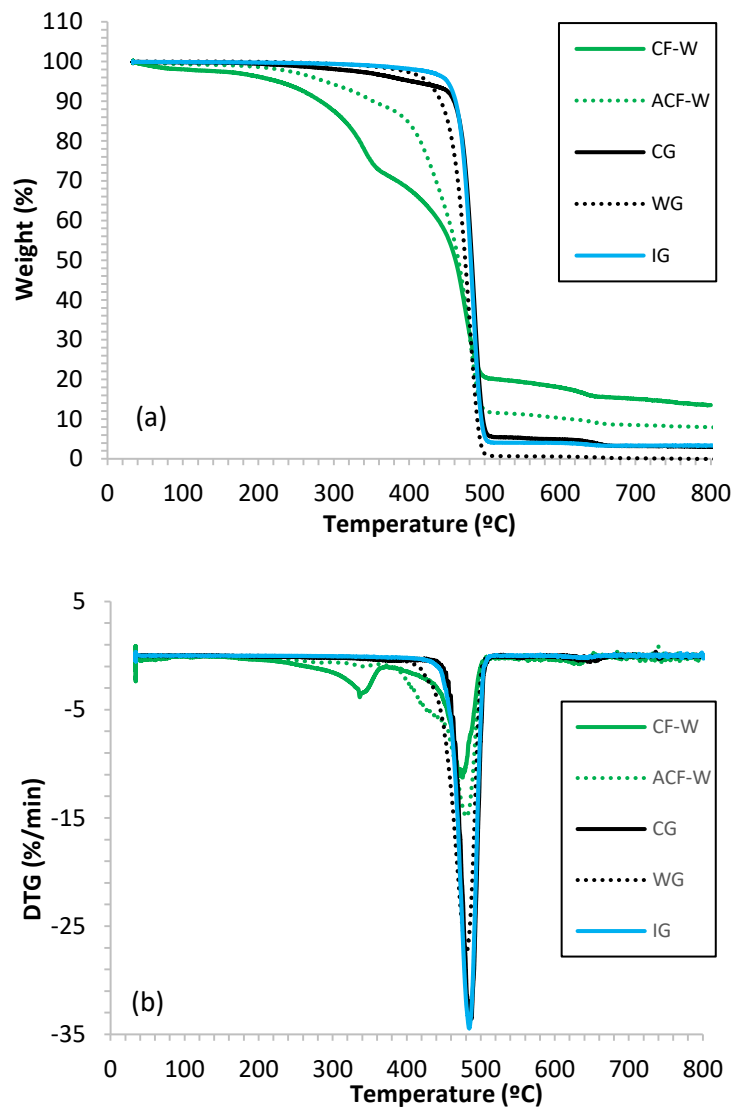
962

963

964

965

966



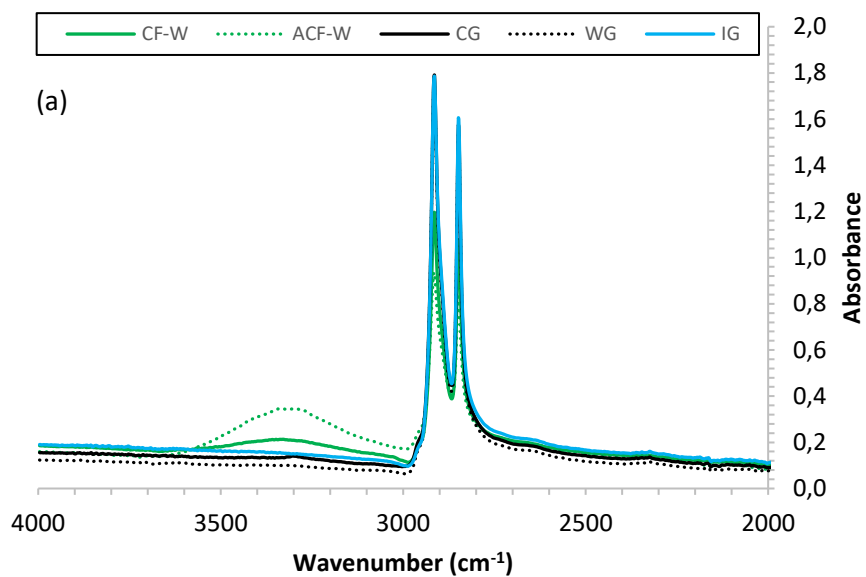
967

968

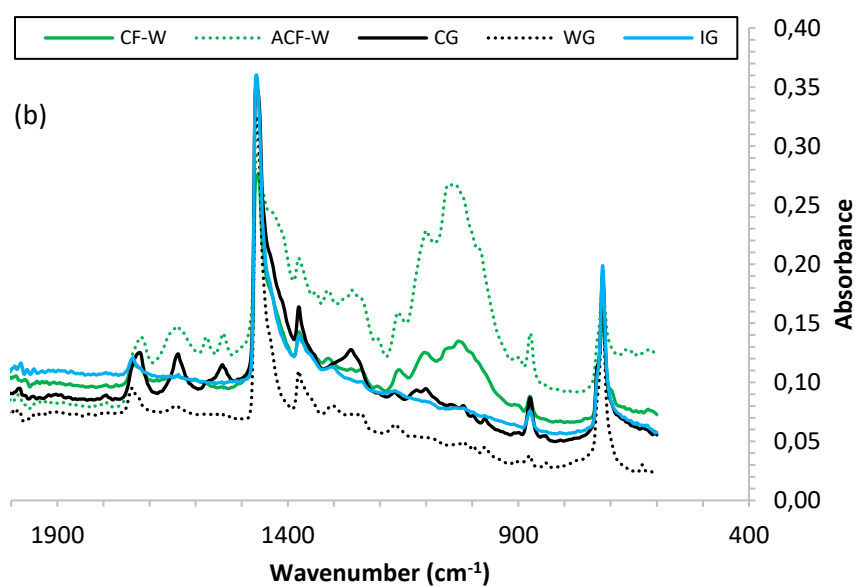
969 **Fig. 1.** TGA-DTG curves obtained in nitrogen flow at $10\text{ }^{\circ}\text{C}\cdot\text{min}^{-1}$ for post-consumer plastic film waste
 970 samples (manual sorting CF-W; automated sorting ACF-W; granules: CG, WG, IG). a) TGA curves; b)
 971 DTG curves.

972

973



974

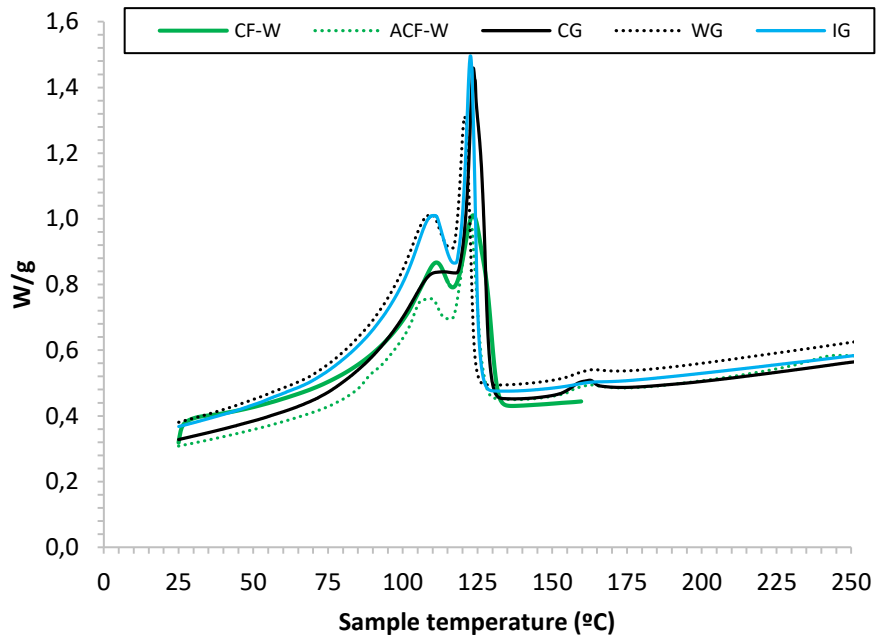


975

976 **Fig. 2.** FT-IR spectra of post-consumer plastic film waste samples (manual sorting CF-W; automated
 977 sorting ACF-W; granules: CG, WG, IG) in the wavenumber range of a) 4000-2000 cm⁻¹ and b) 2000-400
 978 cm⁻¹.

979

980



981

982 **Fig. 3.** DSC scans of post-consumer plastic film waste samples (manual sorting CF-W; automated sorting
 983 ACF-W; granules: CG, WG, IG).

984

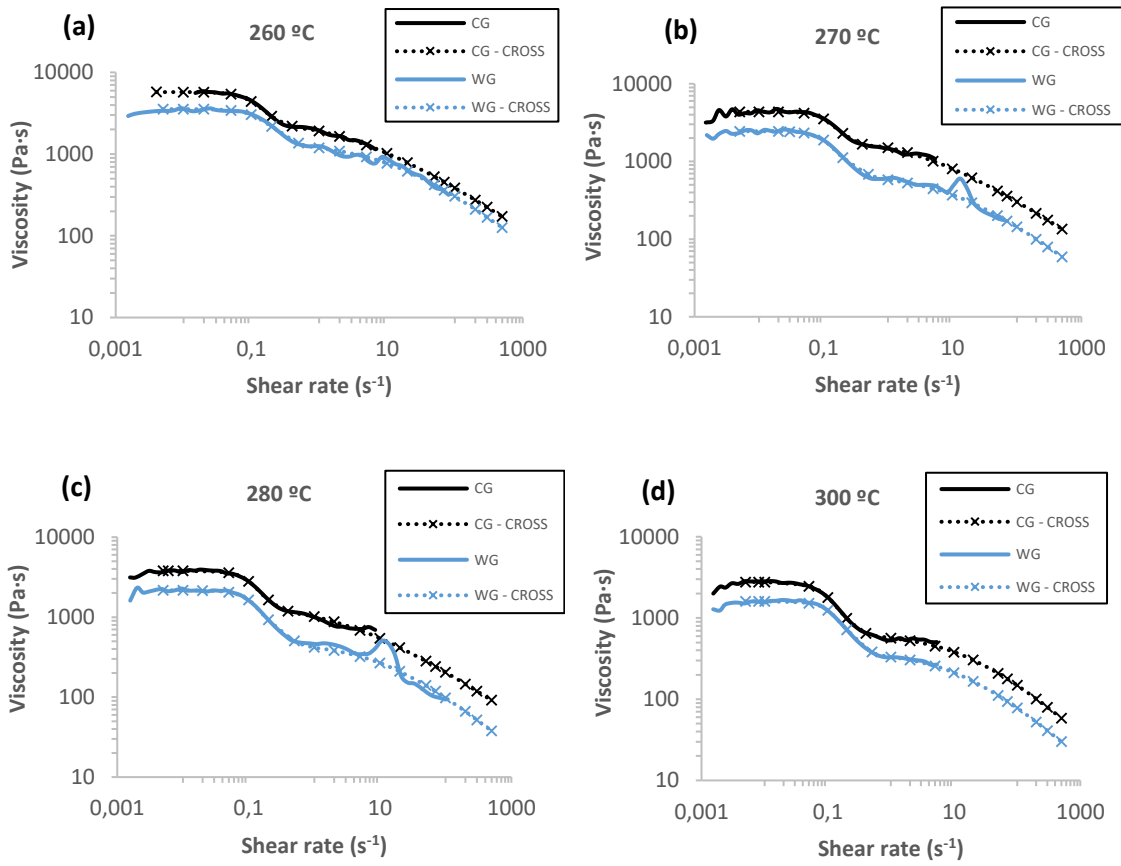
985

986

987

988

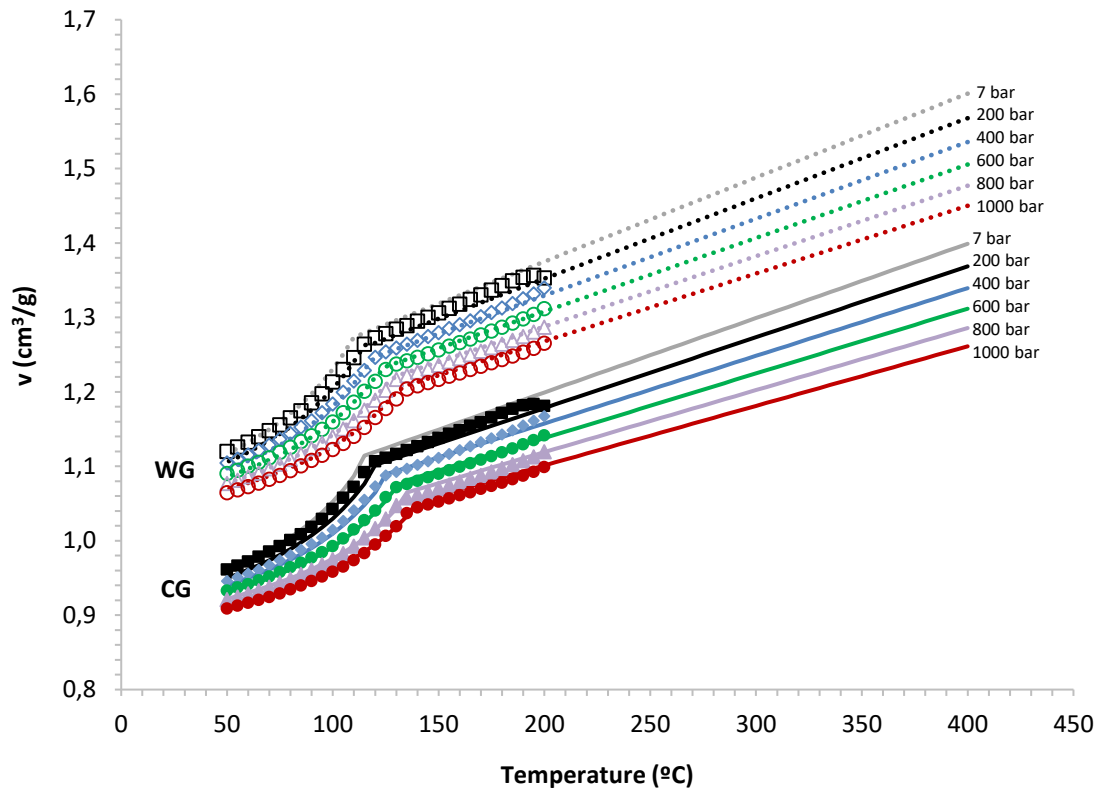
989



990

991

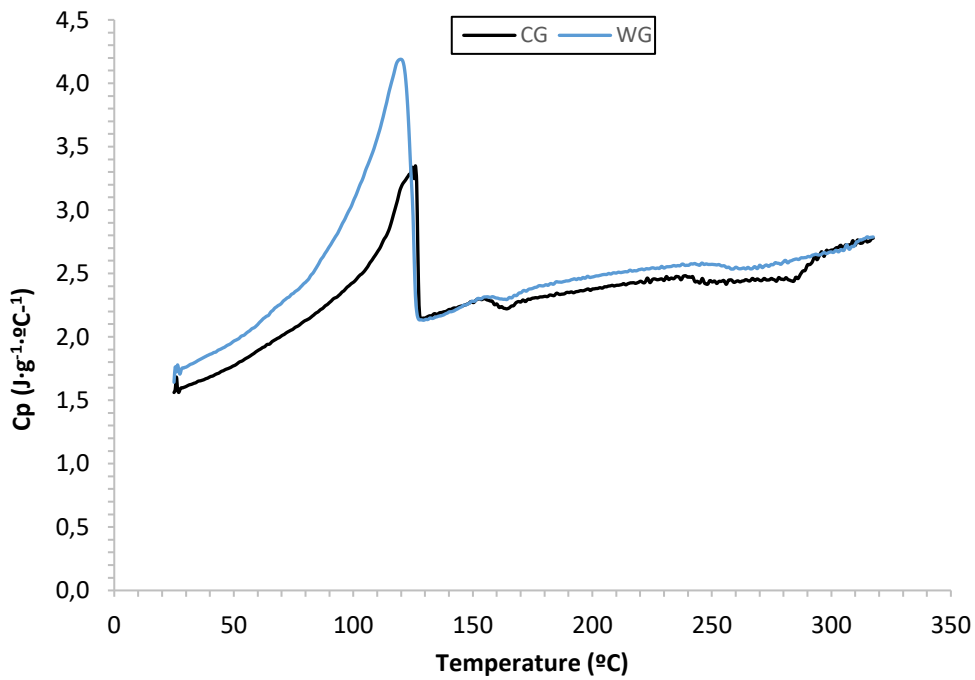
992 **Fig. 4.** Comparison of viscosity curves (solid lines) with Cross model fitting results (dotted lines with
 993 markers) of CG (colour film granules) and WG (white film granules) samples at different temperatures:
 994 (a) 260 °C; (b) 270 °C; (c) 280 °C; (d) 300 °C.



995

996 **Fig. 5.** PVT diagrams (markers) with IKV model fitting results (solid and dotted lines) for CG (colour
 997 film granules) and WG (white film granules).

998



999

1000 **Fig. 6.** Evolution of the specific heat capacity (C_p) as a function of temperature in the range of 25-320 °C
 1001 for CG (colour film granules) and WG (white film granules).